Crystal Structure of Amylose Triacetate I

Yasuhiro Takahashi* and Sumiyo Nishikawa

Department of Macromolecular Science, Graduate School of Science, Osaka University, Toyonaka, Osaka 560-0043, Japan

Received May 27, 2003; Revised Manuscript Received August 8, 2003

ABSTRACT: Amylose triacetate was synthesized by using enzymatically synthesized amylose. The enzymatically synthesized amylose is a linear 1,4-linked poly-α-D-glucose, which does not contain a 1,6-linkage. X-ray crystal structure analysis was carried out for amylose triacetate I. Two left-handed (14/3) helices pass through a unit cell with parameters $a = 10.92$ Å, $b = 18.91$ Å, and c (fiber axis) $= 53.91$ Å and space group $P2_12_12_1$. The molecule does not have 14_{11} symmetry but only has 2_1 symmetry in the crystal. The up- and down-pointing molecules statistically coexist at a crystal site with the ratio 0.87: 0.13. The conformation of the O6 atom is almost tg, but one gg and one gt conformations are included.

Introduction

Amylose is contained about 20−30% in starch, whose chemical structure is an essentially linear (1−4)-α-D-glucan. The properties of amylose are soft and easy to solve in water in contrast with those of cellulose: (1−4)-β-D-glucan. Usually, natural amylose obtained from starch contains a small amount of impurity: amylopectin in addition to a small amount of branch attached by (1−6)-α linkages. On the other hand, enzymatically synthesized amylose used in the present study is purely linear (1−4)-α-D-glucan.[1−3] On the other hand, for amylose triacetate (ATA), two crystalline forms I and II have been found[4−7] and the crystal structures were reported. ATA I assumes left-handed (14/3) helix and two molecular chains pass through a unit cell in antiparallel manner,[6] while ATA II assumes a (9/7) helix.[7] In the present study, the crystal structure of ATA I is reexamined by using linear amylose triacetate synthesized from the enzymatically synthesized amylose.

Experimental Section

Sample. Enzymatically synthesized amylose was kindly supplied by Prof. S. Kitamura of Osaka Prefectural University. Amylose triacetate was synthesized according to the method reported by Jeanes and Jones.[8] The products were examined by elementary analysis and NMR. First, the film was prepared by casting from 4% cloroform solution and was stretched about 3.6 times in a glycerine bath at 170 °C. The fiber specimen was annealed at 180 °C in vacuo for 3 h after fixing on a metal holder. The sample thus obtained is characterized as form I by the following X-ray experiments.

X-ray Measurements. X-ray measurements were carried out by using Cu Kα radiation monochromatized by a pyrolyzed graphite. An imaging plate was used to record the fiber and Weissenberg diagrams, and the intensities were recorded digitally by R-AXIS DSS (Rigaku Denki Co., Ltd.). The fiber diagrams were taken by a cylindrical camera with 5 cm radius in He gas stream. The fiber diagram was shown in Figure 1, which correspond to that of form I.[4−6] The Weissenberg diagrams were taken by a camera with a 4.5 cm radius according to Norman's method (Figure 2).[9] Integrated intensities were estimated by the following procedures,[10] in the same way as by the drum scan densitometer procedures for X-ray films.[11−13] First, digital data for one pixel (100×100 μm^2) of a reflection are summed up along the arc with constant 2θ and the summed intensities are plotted against a layer line. From the one-dimensional intensity curve thus obtained, the integrated intensity was estimated. For the overlapped reflections, one-dimensional curve was fitted and separated under the assumption of a pseudo-Voigt function: a linear combination of Gauss and Cauchy functions.[14] The integrated intensities of 33 reflections including 6 broad reflections were estimated. These reflections were corrected by the Lorentz−polarization factor.

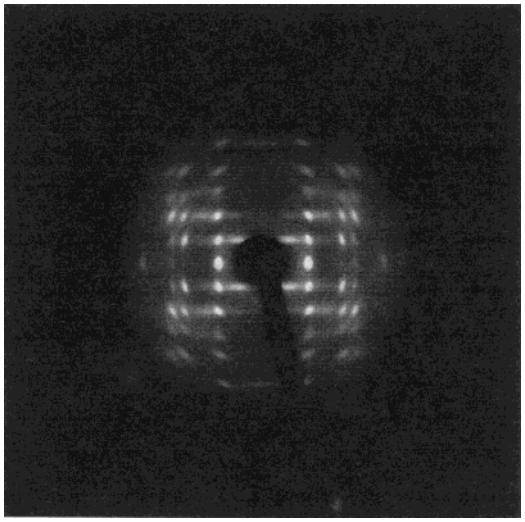

Figure 1. Fiber diagram of amylose triacetate I.

DSC Measurement. DSC measurement was carried out by using DSC-20 (SEIKO Electric Industry Co., Ltd.) in the temperature range 50−300 °C. The melting point 292.6 °C and the glass transition temperature 98 °C were determined.

Density. The density was measured by a flotation method at 25 °C. Small particles of ATA was inserted into a $CaCl_2$ aqueous solution, and water and $CaCl_2$ solution were added alternatively until the particles stopped in the solution. Then, the density of the solution was measured by using DMA500 (Anton Paar).

Results and Discussion

Molecular Conformation. The fiber period is determined as 53.90Å from the reflection 0014 on the Weissenberg diagram (Figure 2). From the whole feature of the fiber diagram, the molecular conformation is considered to be a helix. For a helix, the structure factor is given in cylindrical coordinates as follows[15]

10.1021/ma030288n CCC: $25.00
Published on Web 10/14/2003

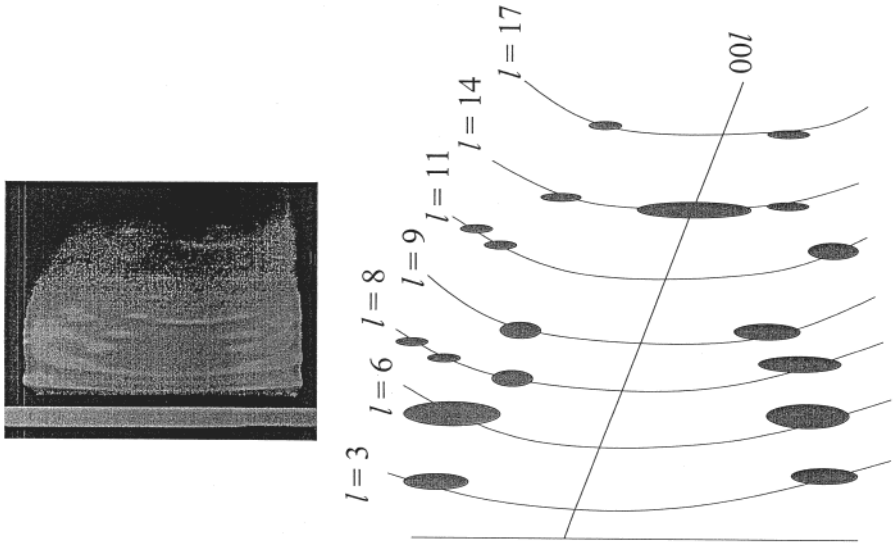

Figure 2. Weissenberg diagram of amylose triacetate I.

$$F(R, \psi, l/c) = \Sigma_n G_{n,l}(R) \exp[in(\psi + \pi/2)] \quad (1)$$

$$G_{n,l}(R) = u\Sigma_j f_j J_n(2\pi R r_j) \exp[i(-n\varphi_j + 2\pi l z_j/c)]$$

$$l = tn + um \quad (2)$$

Here, R, ψ, and l/c are cylindrical coordinates in the reciprocal space; r_j, φ_j, and z_j are the cylindrical coordinates of the jth atom in the real space; f_j is the atomic scattering factor of the jth atom; J_n is the nth order of Bessel function; u and t are the number of units and turns in a fiber identity period; m is an integer. The structure factor is almost represented only by the term including the lowest order of Bessel function obtained by eq 2. The meridional reflections can be observed on the 14th and 28th layer lines. This suggests that these layer lines are composed of the Bessel function with $n = 0$ in eq 1 and $u = 14$ in eq 2. On the other hand, the intensity of the third layer line is strong. This suggests that this layer line is composed of the Bessel function with $n = 1$ in eq 1 and $t = 3$ in eq 2. Accordingly, the molecular conformation is considered to be (14/3) helix. In Table 1, the lowest order of Bessel functions is given for each layer lines.

The molecular models were constructed by using the accepted bond lengths and bond angles[16] (Table 2) for the right-handed and left-handed helices. In Figure 3, a schematic representation of a part of the molecular models is shown, where $h = 3.851$ Å and $\Delta = \pm 77.143°$. And Θ, Φ, and Ψ are the glycosidic bond angle, the internal rotation angle about the bond from the anomeric carbon to the oxygen, and the internal rotation angle about the bond from the glycosylated oxygen to the carbon, respectively. The glycosidic bond angle Θ was assumed to be 110°, and the values reported by Sarko and Marchessault[6] were adopted for the conformation of the acetyl groups in the first stage.

Unit Cell and Space Group. All the observed reflections including 6 broad reflections can be indexed by the orthorhombic unit cell with parameters, a = 10.92 Å, b = 18.91 Å, and c (fiber axis) = 53.90 Å. The density is calculated to be 1.203 g/cm^3 under the assumption that two (14/3) helices pass through a unit cell. This value corresponds well to the observed value of 1.281 g/cm^3.

Table 1. Lowest Order of the Bessel Function for the (14/3) Helix

l	relative intensity[a]	n[b]
0	vs	0
3	vs	1
6	s	2
8	m	−2
9	w	3
11	m	−1
14	w	0
17	w	1

[a] vs = very strong, s = strong, m = moderate, and w = weak. [b] Solutions of $l = 3n + 14m$.

Table 2. Values for Bond Lengths and Bond Angles Used for the Model Building

ring bond lengths (Å)		ring bond angles (deg)	
C4−C3	1.523	C4−C3−C2	110.5
C3−C2	1.521	C3−C2−C1	110.5
C2−C1	1.523	C2−C1−O5	109.2
C4−C5	1.525	C1−O5−C5	114.0
C5−C6	1.514	O5−C5−C4	110.0
O4−C4	1.426	C5−C4−C3	110.3
C3−O3	1.429	O4−C4−C3	110.4
C2−O2	1.423	O4−C4−C5	108.6
C1−O4(2)	1.415	C4−C3−O3	109.7
C1−O5	1.414	C3−C2−O2	110.8
O5−C5	1.436	C2−C1−O4(2)	108.4
C6−O6	1.427	O5−C5−C6	106.9
		C5−C6−O6	111.8
all other lengths (Å)		**all other angles (deg)**	
C−C	1.540	O−C−C	109.5
C−O	1.426	C−O−C	110.0
C═O	1.240	O−C−O	120.0
C−H	1.070		
ring torsion angles (deg)			
O5−C1−C2−C3[a]	56.0	C3−C4−C5−O5	−55.4
C1−C2−C3−C4	−53.2	C4−C5−O5−C1	61.1
C2−C3−C4−C5	53.0	C5−O5−C1−C2	−62.2

[a] Looking from atom 2 to atom 3, the clockwise rotation of bond 3−4 with reference to bond 2−1 is given.

The 27 reflections except for the 6 broad reflections observed on the layer lines show the systematic absences; hkl: $h + k = 2n + 1$ and $00l$: $l = 2n + 1$. This

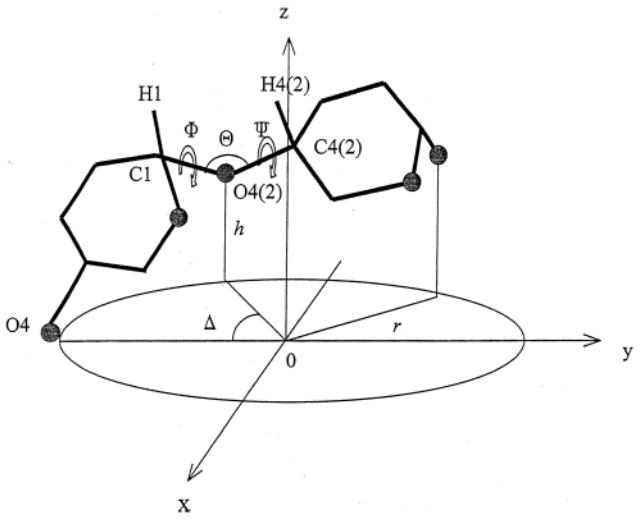

Figure 3. Schematic representation of a part of helical molecule.

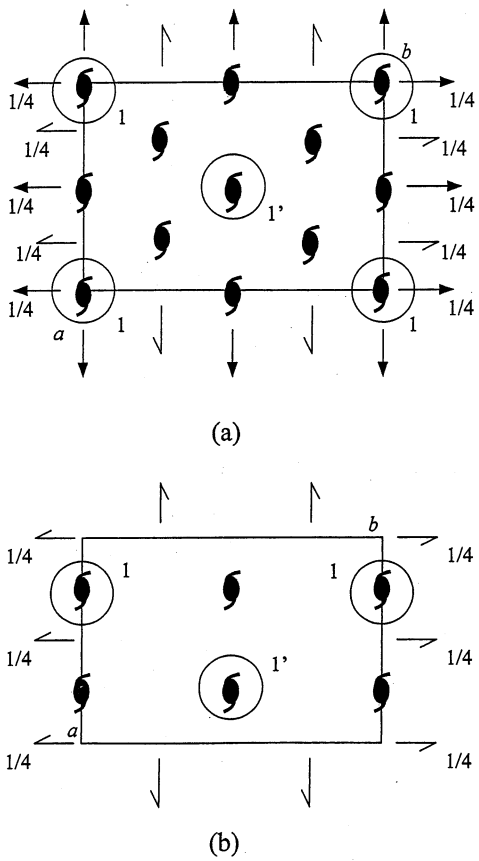

Figure 4. Symmetries of the space groups (a) $C222_1$ and (b) $P2_12_12_1$ and the molecular packings.

shows that the 27 reflections can be interpreted by the space group $C222_1$. On the other hand, all the observed reflections including the 6 broad reflections show the systematic absences; $h00$: $h = 2n + 1$, $0k0$: $k = 2n + 1$, and $00l$: $l = 2n + 1$. This shows that all the observed reflections can be interpreted by the space group $P2_12_12_1$. In Figure 4, the symmetries of the space groups $C222_1$ and $P2_12_12_1$ and the molecular packings are shown. In both space groups, the molecules locate on the 2_1 helical symmetries of the space groups. However, the up- and down-pointing molecules statistically occupy a crystal site with 1:1 ratio in the case of $C222_1$, while,

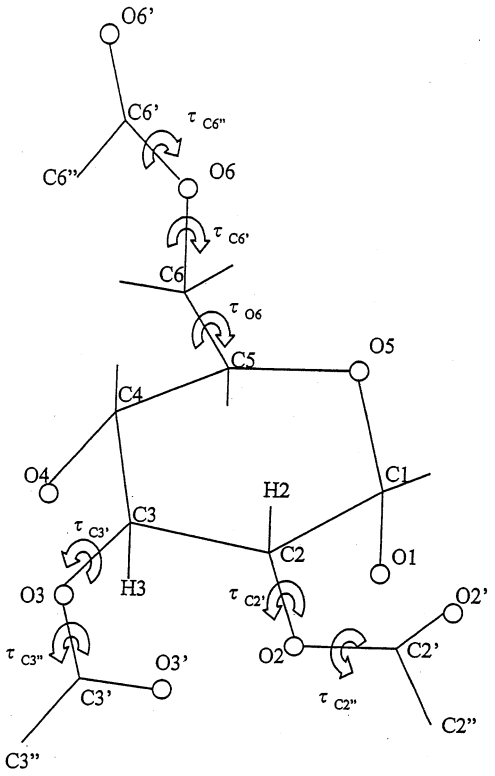

Figure 5. Notation for the internal rotation angles of side chains.

Table 3. Interatomic Distances Fixed by Lagrange's Undetermined Multipliers

atom pair	distance (Å)
C2(1)-O4(2)	2.3837
C1(1)-O4(2)	1.4150
C1(1)-C4(2)	2.3272

in the case of $P2_12_12_1$, only the up- or down-pointing molecule passes through a crystal site. Actually, the existence of the six broad reflections suggests that the space group is $P2_12_12_1$, but the molecular packing is the intermediate between two space groups, i.e., the up- and down pointing molecules, which relate to each other by 2-fold rotation axes perpendicular to the helix axis, statistically occupy a crystal site with different probabilities. This type of molecular packing is already found in the cases of poly(vinylidene fluoride) form II[11] and silk.[13]

Refinements under (14/3) Helical Symmetry. Structural refinements for the right- and left-handed helices were carried out by the constrained least-squares method.[13,17] The variable parameters are the Eulerian angles, θ, φ, and χ, the coordinates of the origin atom, x_0 and y_0, the translation of the molecule along the c-axis z_m, the azimuthal angle of the molecule around the molecular axis φ_m, the isotropic temperature parameter B, the scale factor S, and the internal rotation angles of the branches, τ_{O6}, $\tau_{C6'}$, $\tau_{C6''}$, $\tau_{C3'}$, $\tau_{C3''}$, $\tau_{C2'}$, and $\tau_{C2''}$. Here, the notation for the internal rotation angles of the branches is shown in Figure 5. Lagrange's undetermined multipliers λ were used to keep the interatomic distances between the neighboring residues during the refinement (Table 3). Finally, R factors reduced to 23.5% for the left-handed helix and to 38.8% for the right-handed helix. The results are given in Table 4. In the case of the left-handed helix, the occupancies of the up- and down-pointing molecules are

Table 4. Results Refined under (14/3) Helical Symmetry

model	glucosidic torsion angles[a] (deg) Φ	Ψ	occupancy of disorder	*R* factor
1-left	−48.100	−47.373	0.9:0.1	23.509
1-right	17.307	58.033	1.0:0.0	38.832

[a] The residues are in the (Φ, Ψ) = (0°, 0°) position when the bond sequences H1−C1−O4(2)−C4(2) and C1−O4(2)−C4(2)−H4(2) are cis.

Table 5. Finally Obtained Parameters for Amylose Triacetate I

parameter	value
Cartesian coordinates of origin atom (Å)	
X_0	1.4783
Y_0	−0.2935
Z_0	0.0000
Eulerian angles (deg)	
θ	31.346
ϕ	41.548
χ	−154.387
fractional coordinates of molecule	
translation along the *a*-axis	
x_m	0.2500
translation along the helix axis	
z_m	−0.0304
rotation about the helix axis (deg)	
ϕ_m	−3.985
overall temperature factor (Å^2)	
B	−10.89
occupancy of disorder	
up	0.87
down	0.13
discrepancy factor (%)	
R	14.517

Table 6. Internal Rotation Angles (deg) Finally Obtained for the Side Chains

residue	torsion angles[a] (deg.) τ_{O6}	$\tau_{C6'}$	$\tau_{C6''}$	$\tau_{C3'}$	$\tau_{C3''}$	$\tau_{C2'}$	$\tau_{C2''}$
1	−29 (*gg*)	115	165	140	168	−85	180
2	162 (*tg*)	−164	−170	173	158	−157	180
3	151 (*tg*)	−170	−156	177	115	−129	−172
4	153 (*tg*)	−123	177	140	171	−92	180
5	152 (*tg*)	−172	−167	88	160	−152	170
6	22 (*gt*)	67	132	134	167	168	180
7	151 (*tg*)	−175	−169	133	−179	−161	−178
Sarko et al.[8]	150 (*tg*)	180	180	140 ± 20	180	−130 ± 20	180

[a] τ_{O6}, $\tau_{C3'}$, and $\tau_{C2'}$ are at 0° when the bond sequence of O5−C5−C6−O6, C4−C3−O3−C3′, and C3−C2−O2−C2′ respectively are cis. *tg* means the bond C6−O6 is trans to O5−C5 and *gauche* to C4−C5; *gt* and *gg* are defined correspondingly. Rotation of C6−O6 is positive-clockwise looking from C5 to C6, and pure *tg* = 180°, *gt* = 60°, and *gg* = −60°. When the bond O3−C3′ is cis to H3−C3, $\tau_{C3'} = 120°$, and when the bond O2−C2′ is cis to H2−C2, $\tau_{C2'} = -120°$.

0.9 and 0.1, respectively, while, in the case of the right-handed helix, they are 1.0 and 0.0, respectively. This shows that the left-handed helix structure includes the parallel structure in addition to the antiparallel structure, while the right-handed helix structure is composed only of the antiparallel structure. Anyway, the *R* factors are not sufficiently low to distinguish which model is correct.

Refinements under 2-Fold Screw Symmetry. At the next step, the following model is considered. The molecule is distorted from the (14/3) helical symmetry and only the space group symmetry is kept. Accordingly, seven residues constitute one asymmetric unit, and therefore, the molecule possesses only the 2-fold screw symmetry. In fact, the meridional reflections except for

Table 7. Comparison between the Observed and Calculated Structure Factors

h	*k*	*l*	F_o	F_c	*h*	*k*	*l*	F_o	F_c
0	2	0	917.5	1004.8	1	0	8	-	87.9
1	1	0			0	2	8	282.7	310.5
1	2	0	-	146.3	1	1	8		
1	3	0	232.8	227.4	0	3	8	-	194.1
2	0	0			1	2	8	-	233.1
2	1	0	-	258.5	1	3	8	455.7	500.7
0	4	0	203.4	252.5	2	0	8		
2	2	0			2	1	8	-	300.1
1	4	0	-	132.3	0	4	8	451.7	462.6
2	3	0	-	82.0	2	2	8		
1	5	0			0	1	9	-	67.0
2	4	0	437.3	486.0	1	0	9	146.9	151.7
3	1	0			0	2	9	374.6	358.1
3	2	0	-	13.9	1	1	9		
0	6	0	193.2	193.1	0	1	11	-	16.2
3	3	0			1	0	11	239.3	253.6
2	5	0	-	195.2	0	2	11	363.7	330.4
0	1	3	457.7	386.8	1	1	11		
1	0	3	805.4	450.1	0	3	11	-	72.3
0	2	3	523.7	486.2	1	2	11	-	167.0
1	1	3			1	3	11	621.4	450.9
0	3	3	303.7	357.5	2	0	11		
1	2	3			2	1	11	-	52.8
1	3	3	578.0	614.2	0	4	11	536.4	407.5
2	0	3			2	2	11		
2	1	3	311.5	246.0	0	5	11	-	42.5
0	4	3	376.8	436.4	1	4	11	-	36.5
2	2	3			2	3	11	-	194.6
0	5	3	-	132.2	3	0	11	-	94.5
1	4	3	-	227.3	1	5	11		
2	3	3	-	128.0	2	4	11	218.6	326.3
3	0	3	-	50.2	3	1	11		
1	5	3			0	1	14	-	14.6
2	4	3	229.2	252.8	1	0	14	-	19.6
3	1	3			0	2	14	326.1	367.3
0	1	6	-	0.3	1	1	14		
1	0	6	44.5	315.3	0	3	14	-	207.9
0	2	6	624.1	624.2	1	2	14	-	241.3
1	1	6			2	1	14	-	241.7
1	2	6	564.8	568.1	1	3	14	224.7	234.1
0	3	6			2	0	14		
1	3	6	575.6	565.7	0	4	14	264.4	295.0
2	0	6			2	2	14		
2	1	6	199.3	267.4	0	1	17	-	114.9
0	4	6	672.8	643.9	1	0	17	-	6.0
2	2	6			0	2	17	269.6	279.7
0	1	8	-	154.1	1	1	17		

00*l* with *l* = 14 are not observed. This suggests that the distortion is not so large. Accordingly, the following assumption was made: The pyranose rings possess the structure of (14/3) helical symmetry which is determined in the previous section and only the conformations of acetyl groups are distorted from the (14/3) symmetry. The variable parameters are the Eulerian angles, θ, φ, and χ, the translation of the molecule along the molecular axis z_m, the azimuthal angle of the molecule around the molecular axis φ_m, the temperature parameter B, the scale factor S, and the internal rotation angles of the branches (τ_{O6}, $\tau_{C6'}$, $\tau_{C6''}$, $\tau_{C3'}$, $\tau_{C3''}$, $\tau_{C2'}$, and $\tau_{C2''}$) × 7. The number of the variable parameters is 56 more than the number of the observed reflections 33. Accordingly, a part of the variable parameters is successively refined. At first, the occupancy and one of the three Eulerian angles were fixed. And two Eulerian angles, z_m, φ_m, B, S, and one of the internal rotation angles of branches were refined. The refined internal rotation angle of the branches was successively changed from τ_{O6} in the first residue to $\tau_{C2''}$ in the seventh residue. Finally, the occupancy was refined. These procedures were repeated.

Table 8. Fractional Coordinates Finally Obtained

atom	*x*/*a*	*y*/*b*	*z*/*c*	atom	*x*/*a*	*y*/*b*	*z*/*c*
			a. For the Ring Atoms				
O4	0.383 13	−0.020 91	−0.030 37	O5	0.166 23	−0.126 29	0.005 76
C4	0.337 84	−0.082 16	−0.017 96	C5	0.209 79	−0.066 52	−0.008 10
C3	0.422 68	−0.102 71	0.003 26	C6	0.121 70	−0.055 75	−0.029 45
C2	0.366 83	−0.162 24	0.018 49	O3	0.537 55	−0.125 92	−0.006 46
C1	0.237 98	−0.142 70	0.026 82	O2	0.438 53	−0.176 12	0.039 98
			b. For the Side Chain Atoms				
O6(1)	0.065 93	−0.120 55	−0.036 95	C2′(4)	0.388 66	0.267 20	0.249 21
C6′(1)	−0.062 41	−0.118 19	−0.032 20	C2″(4)	0.360 32	0.310 90	0.272 62
C6″(1)	−0.126 25	−0.178 80	−0.046 23	O3′(4)	0.098 58	0.198 26	0.239 44
C3′(1)	0.635 11	−0.099 86	0.008 55	O2′(4)	0.422 16	0.286 23	0.228 27
C3″(1)	0.755 06	−0.137 42	0.001 36	O6′(4)	0.456 46	−0.155 39	0.184 60
C2′(1)	0.535 82	−0.223 42	0.034 01	O6(5)	0.145 64	−0.050 24	0.248 47
C2″(1)	0.612 68	−0.238 01	0.057 40	C6′(5)	0.072 74	−0.087 41	0.230 82
O3′(1)	0.614 82	−0.053 79	0.024 39	C6″(5)	−0.015 71	−0.035 46	0.218 06
O2′(1)	0.547 21	−0.245 81	0.012 51	C3′(5)	0.570 05	0.123 58	0.276 17
O6′(1)	−0.105 22	−0.071 71	−0.018 49	C3″(5)	0.688 64	0.167 47	0.274 96
O6(2)	0.246 55	0.068 90	0.031 53	C2′(5)	0.694 88	−0.076 57	0.333 00
C6′(2)	0.248 92	0.131 20	0.016 64	C2″(5)	0.777 40	−0.045 22	0.353 39
C6″(2)	0.369 20	0.133 67	0.001 76	O3′(5)	0.461 42	0.142 22	0.274 88
C3′(2)	0.102 56	−0.240 57	0.084 70	O2′(5)	0.696 20	−0.135 65	0.323 03
C3″(2)	0.039 41	−0.309 10	0.076 07	O6′(5)	0.087 03	−0.151 92	0.227 88
C2′(2)	−0.127 92	−0.148 89	0.120 05	O6(6)	−0.035 17	−0.018 10	0.332 54
C2″(2)	−0.134 67	−0.196 06	0.143 29	C6′(6)	−0.061 48	0.029 46	0.352 36
O3′(2)	0.149 71	−0.225 13	0.104 91	C6″(6)	−0.168 64	0.077 95	0.344 93
O2′(2)	−0.209 44	−0.116 19	0.108 88	C3′(6)	0.527 64	−0.181 93	0.364 06
O6′(2)	0.161 62	0.173 07	0.017 19	C3″(6)	0.608 35	−0.246 18	0.357 69
O6(3)	0.384 02	0.018 16	0.106 03	C2′(6)	0.195 55	−0.230 27	0.413 76
C6′(3)	0.479 99	0.033 94	0.088 98	C2″(6)	0.255 35	−0.263 10	0.436 93
C6″(3)	0.506 80	−0.031 60	0.072 92	O3′(6)	0.546 72	−0.131 33	0.378 17
C3′(3)	−0.188 98	0.033 77	0.156 30	O2′(6)	0.086 12	−0.222 49	0.408 30
C3″(3)	−0.275 24	0.098 18	0.156 46	O6′(6)	−0.000 67	0.026 95	0.371 77
C2′(3)	−0.130 25	0.170 49	0.184 71	O6(7)	0.311 19	0.069 85	0.392 13
C2″(3)	−0.197 35	0.169 31	0.209 83	C6′(7)	0.347 18	0.119 22	0.373 51
O3′(3)	−0.185 25	−0.018 69	0.170 08	C6″(7)	0.470 62	0.096 33	0.362 29
O2′(3)	−0.135 76	0.213 43	0.167 36	C3′(7)	0.008 34	−0.197 65	0.435 29
O6′(3)	0.527 47	0.093 50	0.088 89	C3″(7)	−0.059 49	−0.261 67	0.424 21
O6(4)	0.309 98	−0.070 06	0.176 84	C2′(7)	−0.197 46	−0.037 56	0.478 09
C6′(4)	0.350 07	−0.141 72	0.178 17	C2″(7)	−0.236 20	−0.076 57	0.501 91
C6″(4)	0.244 26	−0.191 20	0.170 75	O3′(7)	0.082 19	−0.194 10	0.452 72
C3′(4)	0.145 00	0.235 32	0.222 96	O2′(7)	−0.245 67	0.012 90	0.467 12
C3″(4)	0.116 60	0.311 73	0.214 92	O6′(7)	0.281 12	0.170 79	0.368 75

Finally, the *R* factor reduced to 14.5% for the left-handed helix and to 29.0% for the right-handed helix. Therefore, it is concluded that the left-handed helix is the correct structure. The final parameters except for the internal rotation angles of the branches are given in Table 5. The internal rotation angles of the branches are given in Table 6 in comparison with the values reported by Sarko and Marchessault.[6] The comparison between the observed and calculated structure factors are given in Table 7. The fractional coordinates finally obtained are given in Table 8. The crystal structure of amylose triacetate I is shown in Figure 6, and the molecular structure is shown in Figure 7.

The structure of the pyranose rings possesses the (14/3) helical symmetry. Therefore, the values of Φ and Ψ are the same for all residues and are −48.1° and 47.4°, respectively. On the other hand, the side chains possess only 2-fold screw symmetry of the space group, and therefore, the side chain structures of seven residues forming an asymmetric unit are different. In the structure reported by Sarko and Marchessault,[6] one residue forms an asymmetric unit and, moreover, $\tau_{C6'}$, $\tau_{C6''}$, $\tau_{C3''}$, and $\tau_{C2''}$ were fixed on 180°and only τ_{O6}, $\tau_{C3'}$, and $\tau_{C2'}$ were refined. They concluded that the O6 atom assumes tg (trans−gauche) conformation. However, in the present study (Table 4), the O6 atom of the first residue assumes gg (gauche−gauche) conformation and that of the sixth residue assumes gt (gauche−trans) conformation. Moreover, $\tau_{C6''}$, $\tau_{C3''}$, and $\tau_{C2''}$ can be said to be almost trans conformation (≈180°) but some of $\tau_{C6'}$ are far from the trans conformation. The occupancies of the up- and down-pointing molecules are 0.87 and 0.13, respectively. This suggests that the crystal in-

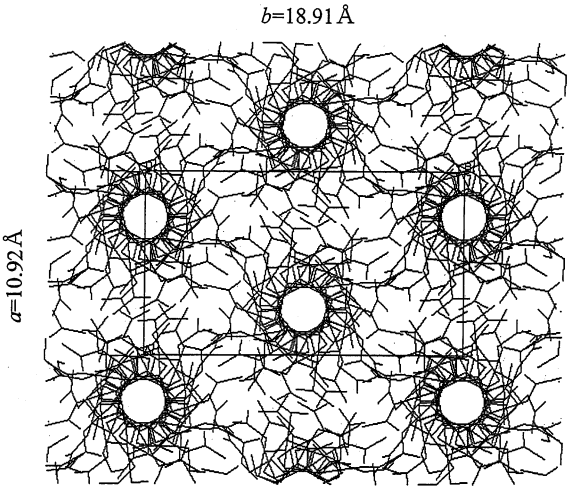

Figure 6. Crystal structure of amylose triacetate I. The up-pointing and down-pointing molecules are described on two crystal sites. Actually, the up-pointing and down-pointing molecules are statistically located on a crystal site with the ratio 0.87:0.13.

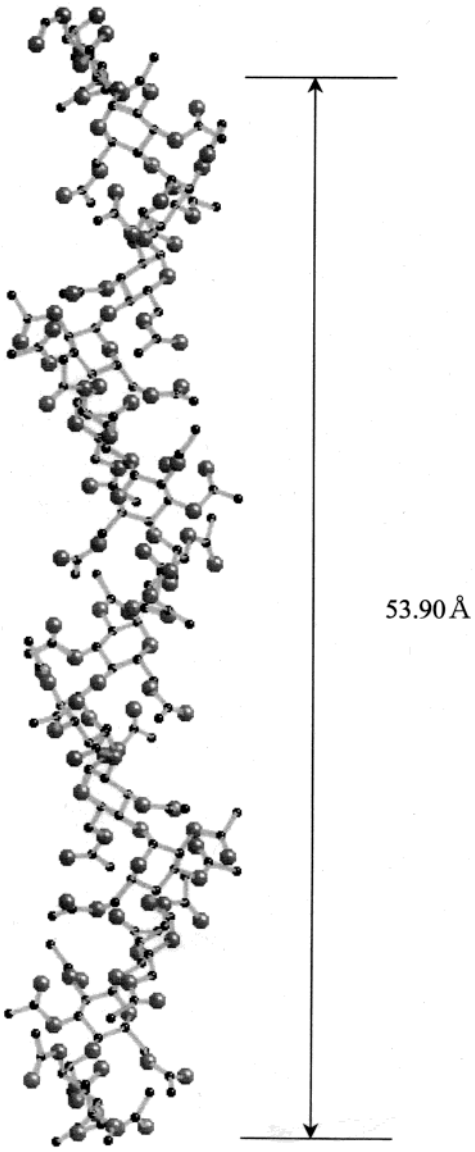

Figure 7. Molecular structure of amylose triacetate I.

Table 9. Short Contacts between Antiparallel Chains

contact	atom pair[a]	atom pair[a]	distance[b] (Å)
1	O5(3)−C3″(13)	C3″(13)−O5(3)	2.887
2	O5(7)−C3″(9)	C3″(9)−O5(7)	2.520
3	C6″(8)−O2(8)	O2(8)-C6″(8)	2.853
4	C6″(8)−C2′(8)	C2′(8)−C6″(8)	2.643
5	C6″(8)−O2′(8)	O2′(8)−C6″(8)	2.988
6	O6(8)−C2″(8)	C2″(8)−O6(8)	2.938
7	O6(8)−C2′(8)	C2′(8)−O6(8)	2.973

[a] The number in parentheses is the sequence number of the monomer residue, counting from the bottom of the unit cell up. For the explanation of atom designations within a monomer residue, refer to Figure 5. [b] Minimum accepatble distance for all following short contacts is 3.15 Å.

cludes not only the antiparallel structure but also the parallel structure. Furthermore, the existence of the broad reflections, which cannot be indexed by the space group $C222_1$, suggests that a kind of superlattice structure exists in the crystallite. In the case of poly-

Table 10. Short Contacts between Parallel Chains

contact	atom pair	atom pair	distance[a] (Å)
1	O6′(2)−O2′(1)	O2′(8)−O6′(9)	1.995
2	O6′(2)−C2′(1)	C2′(8)−O6′(9)	2.558
3	O6′(2)−C2″(1)	C2″(8)−O6′(9)	2.795
4	O6′(3)−C3″(2)	C3″(9)−O6′(10)	1.972
5	O2′(3)−C6″(4)	C6″(11)−O2′(10)	2.237
6	O2′(3)−C6′(4)	C6′(11)−O2′(10)	2.805
7	C3″(4)−O6′(4)	O6′(11)−C3″(11)	2.474
8	O2′(4)−O6′(5)	O6′(12)−O2′(11)	2.148
9	O2′(4)−C6′(5)	C6′(12)−O2′(11)	2.904
10	C2′(4)−O6′(5)	O6′(12)−C2′(11)	2.891
11	O6′(7)−C3″(6)	C3″(13)−O6′(14)	2.526
12	C6″(8)−C2′(6)	C2′(13)−C6″(1)	2.860
13	C6″(8)−C2″(6)	C2″(13)−C6″(1)	2.005
14	C6″(8)−C3″(7)	C3″(14)−C6″(1)	2.815
15	C6″(8)−C3′(7)	C3′(14)−C6″(1)	2.848
16	C6″(8)−O3′(7)	O3′(14)−C6″(1)	2.452

[a] Minimum acceptable distances for O−O, C−O, and C−C following short contacts are 2.80, 3.15, and 3.50 Å, respectively.

(vinylidene fluoride), the superlattice structure is the antiphase domain structure.[18]

The intermolecular atom−atom distances were calculated. The short contacts for antiparallel chains and parallel chains are given in Tables 9 and 10, respectively. Some of them are too short, but, they are reasonably acceptable from the accuracy of the present study. The parallel chains give short contacts more than the antiparallel chains. This corresponds well to the fact that the antiparallel component in crystal is dominant to the parallel component.

Acknowledgment. The authors express their thanks to Prof. S. Kitamura of Osaka Prefectural University for supplying the enzymatically synthesized amylose.

References and Notes

(1) Kitamura, S.; Yunokawa, H.; Mitsuie, S.; Kuge, T. *Polym. J.* **1982**, *14*, 93.
(2) Kitamura, S. *Polymeric Materials Encyclopedia*; Salomone, J. C., Ed.; CRC Press: New York, 1996; Vol. 10, p 7915.
(3) Nakanishi, Y.; Norisue, T.; Teramoto, A. *Macromolecules* **1993**, *26*, 4220.
(4) Whistler, R. L.; Schieltz, N. C. *J. Am. Chem. Soc.* **1943**, *65*, 1436.
(5) Sarko, A.; Marchessault, R. H. *Science* **1966**, *154*, 1658.
(6) Sarko, A.; Marchessault, R. H. *J. Am. Chem. Soc.* **1967**, *89*, 6454.
(7) Zugenmaier, P.; Steinmeier, H. *Polymer* **1986**, *27*, 1601.
(8) Jeanes, A.; Jones, R. W. *J. Am. Chem. Soc.* **1952**, 74, 6116.
(9) Norman, N. *Acta Crystallogr.* **1954**, *7*, 462.
(10) Takahashi, Y.; Sul, H. To be published.
(11) Takahashi, Y.; Matsubara, Y.; Tadokoro, H. *Macromolecules* **1982**, *15*, 334.
(12) Takahashi, Y.; Ozaki, Y.; Takase, M.; Krigbaum, W. R. *J. Polym. Sci., Part B: Polym. Phys.* **1993**, *31*, 1135.
(13) Takahashi, Y.; Gehoh, M.; Yuzuriha, K. *Int. J. Biol. Macromol.* **1999**, *24*, 127.
(14) Takahashi, Y.; Ishida, T. *J. Polym. Sci., Part B: Polym. Phys.* **1988**, *26*, 2267.
(15) Cochran, W.; Crick, C.; Vand, V. *Acta Crystallogr.* **1952**, *5*, 581.
(16) Arnott, S.; Scott, W. E. *J. Chem. Soc., Perkin Trans. II* **1972**, 324.
(17) Takahashi, Y.; Sato, T.; Tadokoro, H.; Tanaka, Y. *J. Polym. Sci., Polym. Phys. Ed.* **1973**, *11*, 223.
(18) Takahashi, Y.; Tadokoro, H. *Macromolecules* **1983**, *16*, 1880.

MA030288N